Unpaired Spin Populations and Spin-Pairing Tendencies of the Nonequivalent Vanadium Sites of the Magnetic Metal NaV_6O_{11} Investigated by Electronic Band Structure Calculations and Spin Dimer Analysis

A. Villesuzanne*,† and M.-H. Whangbo*

Department of Chemistry, North Carolina State University, Raleigh, North Carolina 27695-8204

H.-J. Koo*

Department of Chemistry and Institute for Basic Science, Kyung Hee University, Seoul 130-701, South Korea

Received March 28, 2005. Revised Manuscript Received June 14, 2005

The unpaired spin populations and spin-pairing tendencies of the three different vanadium atoms of NaV_6O_{11} above and below its trimerization temperature $T_t = 245$ K were examined by determining, as a function of the number of unpaired spins per formula unit, N, the total energies of NaV_6O_{11} as well as the 3d orbital populations of the V(1), V(2), and V(3) atoms on the basis of first-principles spin-polarized electronic band structure calculations. Spin dimer analysis was also carried out to estimate the spin-pairing tendencies of the V(1) and V(2) sites above and below T_t. Our work does not support the heuristic assumptions employed to interpret the magnetic properties of NaV_6O_{11} as well as its analogues SrV_6O_{11} and PbV_6O_{11}. States with a wide range of N values (i.e., $\sim 4 < N < \sim 9$) are expected to contribute to the magnetic properties of NaV_6O_{11} above and below T_t. The V(1), V(2), and V(3) atoms differ mainly in the extents of their spin polarizations but not in their oxidation states. The unpaired spin population of each V(1) site is significantly reduced by the trimerization but remains nonzero below T_t. The V(2) sites, which are present as dimer units, are not diamagnetic. The V(2) and V(3) sites each have approximately one unpaired spin per site above and below T_t.

1. Introduction

NaV_6O_{11} is a magnetic metal with anomalous magnetic and electrical properties and undergoes two structural phase transitions. The crystal structure of NaV_6O_{11}[1−3] consists of the V_3O_8 layers of face-sharing $V(1)O_6$ octahedra, the V_2O_9 dimers of face-sharing $V(2)O_6$ octahedra, and the $V(3)O_5$ trigonal bipyramids (Figure 1). These structural units share their oxygen corners to form the three-dimensional (3D) lattice of NaV_6O_{11}, in which the V(1) atoms of each V_3O_8 layer form a kagomé lattice (Figure 2a). Two structural phase transitions take place at 245 and 80 K, and a ferromagnetic transition takes place at 60 K.[2−5] The occurrence of the three phase transitions in NaV_6O_{11} was confirmed by specific heat experiments.[4] The main structural change associated with the phase transition at 245 K is a trimerization of the V(1) atoms in each kagomé lattice (Figure 2b). NaV_6O_{11} shows a metallic behavior at all temperatures along the direction perpendicular to the V_3O_8 layer, that is, parallel to the c-axis (hereafter referred to as the parallel direction). Along any direction perpendicular to the c-axis (hereafter referred to as the perpendicular direction), NaV_6O_{11} is metallic above 245 K and below 80 K, and its resistivity is very weakly semiconducting (nearly temperature-independent) between these two temperatures. The electrical resistivity is lower along the parallel than along the perpendicular direction in the whole temperature range studied (i.e., $\rho_{\parallel} < \rho_{\perp}$).[6,7] The

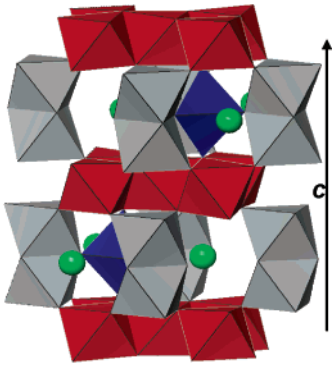

Figure 1. Polyhedral view of the crystal structure of NaV_6O_{11}. The red, gray, and blue polyhedra represent the $V(1)O_6$ octahedra, the $V(2)O_6$ octahedra, and the $V(3)O_5$ trigonal bipyramids, respectively. The green spheres represent the Na atoms.

* E-mails: ville@icmcb-bordeaux.cnrs.fr (A.V.); mike_whangbo@ncsu.edu (M.-H.W); hjkoo@khu.ac.kr (H.-J.K).

† Permanent address: ICMCB-CNRS, 87 Av. Dr. Schweitzer, 33608 Pessac cedex, France.

(1) De Roy, M. E.; Besse, J. P.; Chevalier, R.; Gasperin, M. *J. Solid State Chem.* **1985**, *67*, 185.
(2) Kanke, Y.; Kato, K.; Takayama-Muromachi, E.; Isobe, M. *Acta Crystallogr., Sect. C* **1992**, *48*, 1376.
(3) Kanke, Y.; Izumi, F.; Morii, Y.; Akiba, E.; Funahashi, S.; Kato, K.; Isobe, M.; Takayama-Muromachi, E.; Uchida, Y. *J. Solid State Chem.* **1994**, *112*, 429.
(4) Akiba, A.; Yamada, H.; Matsuo, R.; Kanke, Y.; Haeiwa, T.; Kita, E. *J. Phys. Soc. Jpn.* **1998**, *67*, 1303.
(5) Iwata, M.; Ishibashi, Y. *J. Phys. Soc. Jpn.* **1998**, *67*, 691.

10.1021/cm050666y CCC: $30.25
Published on Web 07/26/2005

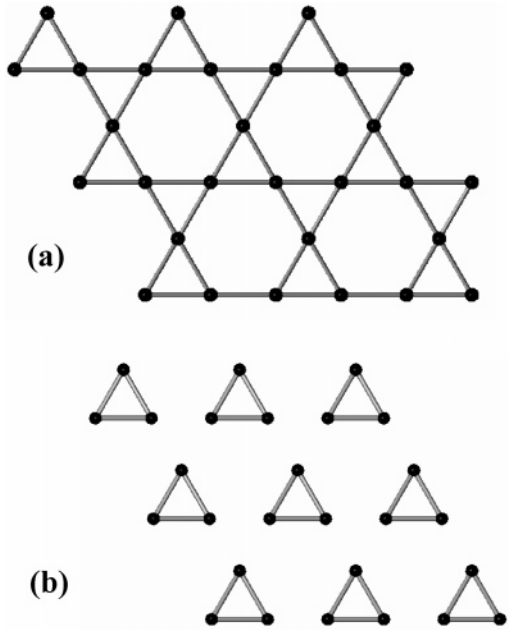

Figure 2. Arrangements of the V(1) atoms in the $V(1)_3O_8$ layers of NaV_6O_{11} (a) above and (b) below the trimerization temperature 245 K.

electronic structure and metallic properties of NaV_6O_{11} were examined on the basis of extended Hückel tight-binding (EHTB) electronic structure calculations.[8]

The magnetic susceptibilities of NaV_6O_{11} as well as its isostructural analogues SrV_6O_{11} and PbV_6O_{11} show a similar temperature dependence, with a Curie−Weiss behavior above the trimerization temperature T_t and a ferromagnetic ordering below T_C (i.e., $T_t = 245$, 320, and 560 K and $T_C = 65$, 75, and 85 for NaV_6O_{11}, SrV_6O_{11}, and $PbV6O_{11}$, respectively).[9] In interpreting results of their magnetic susceptibility measurements, Kato et al.[9] introduced three simplifying assumptions: (a) the V(1), V(2), and V(3) atoms have the oxidation states +3, +4, and +4, respectively, so that they possess two, one, and one d-electron, respectively, (b) the V(2) sites are nonmagnetic at all temperatures because of the pairing of the d electrons in each V_2O_9 dimer, and (c) the spin state of the V(1) sites changes from $S = 1$ to $S = 0$ below T_t because of the spin pairing associated with the trimerization in the V_3O_8 layers. In this picture, only the d electrons of the VO_5 trigonal bipyramids remain to participate in the ferromagnetic ordering in the metallic state below T_C. By introducing an additional assumption that thermal excitations take place below T_t through a forbidden energy gap between the spin singlet and triplet states of the V(1) sites, Kato et al.[10] were able to fit the magnetic susceptibility and ^{23}Na NMR data of NaV_6O_{11} with parameters consistent with the experimental data. They suggested that the spin-state transition of V(1) from a paramagnetic to a spin singlet state below T_t is analogous to the paramagnetic-to-nonmagnetic phase transition found for the hexagonal lattice of V^{3+} (d^2) ions in each VO_2 layer of $LiVO_2$,[11] which is understood in terms of either second-order Jahn−Teller effect,[8] charge-density wave (CDW) formation,[11,12] or orbital ordering.[13]

Kato et al.'s assumptions are undoubtedly useful in simplifying the interpretation of the physical properties of NaV_6O_{11}. However, whether their assumptions are valid on theoretical basis has not been tested so far. Furthermore, it is difficult to accommodate the observed metallic properties of NaV_6O_{11} in terms of their assumptions. To find a sound theoretical basis for interpreting the apparently puzzling magnetic and transport properties of NaV_6O_{11}, it is necessary to examine its electronic structure above and below its trimerization temperature T_t. Thus, we investigated the unpaired spin populations of the V(1), V(2), and V(3) atoms in the room temperature (RT) and 200 K crystal structures of NaV_6O_{11} on the basis of first-principles spin-polarized electronic band structure calculations, and we estimated the spin-pairing tendencies of the V(1) and V(2) sites in terms of spin dimer analysis on the basis of EHTB calculations.

2. Computational Details

Density functional theory spin-polarized electronic band structure calculations were carried out to examine the electronic structures for the RT and 200 K crystal structures of NaV_6O_{11}. We first performed all-electron calculations, using the augmented plane wave plus local orbitals method (APW+lo)[14,15] implemented in the WIEN2k code[16] with the generalized gradient approximation (GGA) of Perdew et al. for the exchange-correlation energy.[17] Atomic sphere radii were 1.8, 1.8, and 1.5 au for Na, V, and O, respectively. The plane-wave cutoff was $R_{MT} \cdot K_{max} = 7$, and the irreducible wedge of the Brillouin zone was sampled with a 42 k-points mesh.

Although self-consistent-field (SCF) convergence was achieved successfully, the 200 K structure was calculated to be less stable than the RT structure by 1.3 eV per formula unit (FU), indicating that the SCF convergence led to a local minimum for the 200 K structure. Therefore, we chose to examine in some detail the full range of possible unpaired spin populations for NaV_6O_{11}, from the nonpolarized to the fully polarized 3d bands (i.e., from 0 to 9 unpaired electrons per FU), by performing first-principles pseudo-potential calculations. We used the VASP code[18] with the GGA of

(6) Kanke, Y.; Takayama-Muromachi, E.; Kato, K.; Matsui, Y. *J. Solid State Chem*. **1990**, *89*, 130.
(7) Uchida, Y.; Kanke, Y.; Takayama-Muromachi, E.; Kato, K. *J. Phys. Soc. Jpn*. **1991**, *60*, 2530.
(8) Seo, D.-K.; Whangbo, M.-H. *J. Am. Chem. Soc*. **1996**, *118*, 3951.
(9) Kato, H.; Kato, M.; Yoshimura, K.; Kosuge, K. *J. Phys.: Condens. Matter* **2001**, *13*, 9311.
(10) Kato, H.; Kato, M.; Yoshimura, K.; Kosuge, K. *J. Phys. Soc. Jpn*. **2001**, *70*, 1404.
(11) Goodenough, J. B.; Dutta, G.; Manthiram, A. *Phys. Rev. B* **1991**, *43*, 10170.
(12) (a) Rovira, C.; Whangbo, M.-H. *Inorg. Chem*. **1993**, *32*, 4094. (b) Whangbo, M.-H.; Canadell, E. *J. Am. Chem. Soc*. **1992**, *114*, 9587.
(13) Pen, H. F.; van den Brink, J.; Khomskii, D. I.; Sawatsky, G. A. *Phys. Rev. Lett*. **1997**, *78*, 1323.
(14) Sjöstedt, E.; Nordström, L.; Singh, D. J. *Solid State Commun.* **2000**, *114*, 15.
(15) Madsen, G. K. H.; Blaha, P.; Schwarz, K.; Sjöstedt, E.; Nordström, L. *Phys. Rev. B* **2001**, *64*, 195134.
(16) Blaha, P.; Schwarz, K.; Madsen, G.; Kvasnicka, D.; Luitz, J. *WIEN2k, An Augmented Plane Wave + Local Orbitals Program for Calculating Crystal Properties*; Techn. Universität Wien, 2001; ISBN 3-9501031-1-2; see also: http://www.wien2k.at/.
(17) Perdew, J. P.; Burke, S.; Ernzerhof, M. *Phys. Rev. Lett*. **1996**, *77*, 3865.
(18) Kresse, G.; Furthmüller, J. *Phys. Rev. B* **1996**, *54*, 11169; *Comput. Mater. Sci*. **1996**, *6*, 15; see also: http://cms.mpi.univie.ac.at/vasp/.

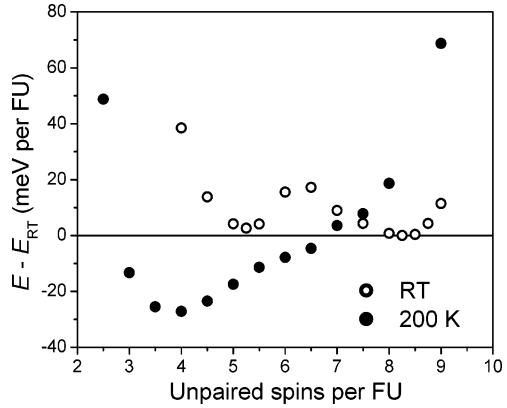

Figure 3. Relative energies calculated for the RT and 200 K crystal structures of NaV_6O_{11} as a function of the number of unpaired spins per formula unit, *N*.

Perdew and Wang[19] and the projected augmented wave method[20,21] for the valence-ion core interactions. The energy cutoff for the plane-wave basis set was 400 eV, and 32 k-points were used for the sampling of the Brillouin zone.

The spin-pairing tendencies for the d electrons of the V(1) atoms in the V_3O_8 layers and those of the V(2) atoms in the V_2O_9 dimers were estimated by performing spin dimer analysis[22] for the V(1)···V(1) and V(2)···V(2) interactions in the crystal structures of NaV_6O_{11} on the basis of EHTB calculations.[23] The 3d orbitals of V and the 2s/2p orbitals of O were represented by double-ζ Slater type orbitals.[24]

3. Electronic Structures above and below the Trimerization Temperature

3.1. Total Energy as a Function of the Unpaired Spin Population per Formula Unit. The total energies of the RT and 200 K crystal structures were calculated as a function of the number of unpaired spins per FU, *N*. Our results are summarized in Figure 3, where the total energies are given in terms of the relative energies ΔE with the lowest energy of the RT structure as the energy reference. The ΔE-versus-*N* curve for the RT crystal structure shows two minima at $N = 5.25$ and 8.25. The d-block bands of NaV_6O_{11} have nine electrons per FU, so that the $N > 9$ states involve a spin-polarization of the oxygen 2p-block bands in addition to that of the vanadium d-block bands. Thus, the $N > 9$ states are less stable than the ground state ($N = 8.25$) by more than 1.4 eV. The $N = 3$ state lies 190 meV above the ground state. The two minimum-energy states ($N = 5.25$ and 8.25) differ in energy by less than 3 meV per FU and are separated by an energy barrier lower than 20 meV per FU. Above T_t, therefore, the thermal populations of the states around $N = 5.25$ cannot be neglected compared with those of the states around $N = 8.25$.

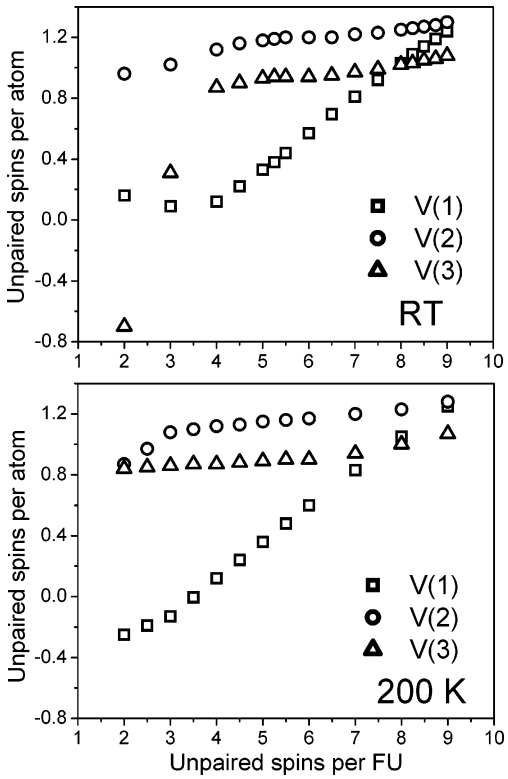

Figure 4. Unpaired spin populations of the V(1), V(2), and V(3) atoms calculated for the ground states of the RT and 200 K crystal structures of NaV_6O_{11} as a function of the number of unpaired spins per formula unit, *N*.

For the 200 K structure, independent fixed-spin-moment calculations led to a ΔE-versus-*N* curve with a large discontinuity in the region of $N = 4-5$ (see Figure S1 of the Supporting Information). By starting with the wave functions calculated at the point of discontinuity and varying the fixed moment gradually, it was possible to establish the two distinct ΔE-versus-*N* curves. It is the lower-energy curve that is presented in Figure 3. At a given *N*, the energy point of the lower-energy curve corresponds to the global minimum energy and that of the upper-energy curve corresponds to a local minimum energy. Our discussion for the 200 K structure given below is based on the global minimum-energy curve. For the 200 K structure, the ΔE-versus-*N* curve shows a minimum at $N = 4$, which lies approximately 30 meV per FU below the ground state of the RT structure ($N = 8.25$). The comparison of the ΔE-versus-*N* curves for the RT and 200 K structures reveals that the trimerization stabilizes the states around $N = 4$ and destabilizes those around $N > 7$ and converts the double-well energy curve into a single-well energy curve. Nevertheless, at 200 K, the states with $N \geq 4$ lie within a small energy difference from the ground state. For example, the energy difference between the ground and the $N = 6$ states is smaller than 20 meV.

3.2. d-Orbital and Spin Populations on the Three Nonequivalent Vanadium Sites. How the unpaired spin populations μ on the V(1), V(2), and V(3) atoms vary as a function of *N* is summarized in Figure 4a for the RT structure and in Figure 4b for the 200 K structure. Although the ΔE-versus-*N* curves for the two structures are quite different (Figure 3), the μ-versus-*N* curves for the two structures are nearly identical in the range of $N = 4-9$. The unpaired spin

(19) Perdew, J. P.; Wang, Y. *Phys. Rev. B* **1992**, *45*, 13244.
(20) Blöchl, P. E. *Phys. Rev. B* **1994**, *50*, 17953.
(21) Kresse, G.; Joubert, J. *Phys. Rev. B* **1999**, *59*, 1758.
(22) Whangbo, M.-H.; Koo, H.-J.; Dai, D. *J. Solid State Chem.* **2003**, *176*, 417, and the references therein.
(23) Our calculations were carried out by employing the SAMOA (Structure and Molecular Orbital Analyzer) program package (Dai, D.; Ren, J.; Liang, W.; Whangbo, M.-H. http://chvamw.chem.ncsu.edu/ (accesesed 2002)).
(24) Clementi, E.; Roetti, C. *At. Data Nucl. Data Tables* **1974**, *14*, 177.

Table 1. Up-Spin, Down-Spin, and Net-Spin 3d Orbital Populations of the V(1), V(2), and V(3) Atoms Calculated for the RT and 200 K Crystal Structures of NaV_6O_{11}

		up spin	down spin	net spin
V(1)	RT ($N = 8.25$)	1.65	0.56	1.09
	RT ($N = 5.25$)	1.29	0.91	0.38
	200 K ($N = 4.00$)	1.15	1.03	0.12
V(2)	RT ($N = 8.25$)	1.73	0.47	1.26
	RT ($N = 5.25$)	1.70	0.51	1.19
	200 K ($N = 4.00$)	1.65	0.54	1.11
V(3)	RT ($N = 8.25$)	1.62	0.59	1.03
	RT ($N = 5.25$)	1.57	0.63	0.94
	200 K ($N = 4.00$)	1.53	0.66	0.87

population of V(2) varies little with N, that is, 1.1−1.3 in the region of $N = 4-9$ at temperatures above and below T_t. This is not in support of the assumption[9,10] that V(2) is nonmagnetic below 245 K. The unpaired spin population of V(3) varies little with N as well, that is, 0.8−1.0 in the region of $N = 4-9$ at temperatures above and below T_t. The latter supports the assumption[10] that the V(3) site has one unpaired spin above and below T_t. With decreasing N, the unpaired spin population of V(1) decreases sharply from 1.0 at $N =$ 9 to 0.12 at $N = 4$. Namely, although the unpaired spin population of the V(1) site is strongly diminished, it does not vanish upon the trimerization. This does not support the assumption that the V(1) site becomes diamagnetic below T_t. Thus, the V(1) site cannot be described by a simple spin-pairing picture that predicts an energy gap below T_t.

The μ-versus-N curve of the RT structure (Figure 4a) reveals that the decrease in N arises primarily from that in the unpaired spin population of V(1). At RT, that is, at the temperature well above T_t, the states around $N = 5.25$ are only slightly higher in energy than the ground state ($N =$ 8.25), so that the effective number of unpaired spins per FU above T_t should be smaller than 8.25 because of the thermal populations of the lower unpaired-spin-population states around $N = 5.25$. Similarly, the effective number of unpaired spins per FU below T_t should be greater than four because of the thermal populations of the higher unpaired-spin-population states of $N \geq 4$. These "thermal excitations" into the low-lying excited states are gapless excitations and differ from the model of gapped excitations introduced by Kato et al.[10] to explain the nonlinear behavior of the χ^{-1}-versus-T curve and the NMR spin−lattice relaxation rate below T_t.

At RT, the unpaired spin population of V(1) for the states around $N = 5.25$ is only 0.38, which is not far from 0.12 found for the ground state of the 200 K structure (Table 1). Thus, even in the absence of the trimerization distortion, the electronic structures of the lower unpaired-spin-population states around $N = 5.25$ show that the d electrons of the V(1) sites in the V_3O_8 layers of NaV_6O_{11} have significant spin pairing in the V(1)···V(1) contacts. Thermal occupations of the lower unpaired-spin-population states around $N = 5.25$ should act as a driving force for the trimerization of NaV_6O_{11}.

The total 3d orbital populations of the V(1), V(2), and V(3) atoms calculated for their atomic spheres are in the range of 2.19−2.21 electrons for the RT and the 200 K structures for all different N values. As representative examples, Table 1 lists the up-spin, down-spin, and net-spin

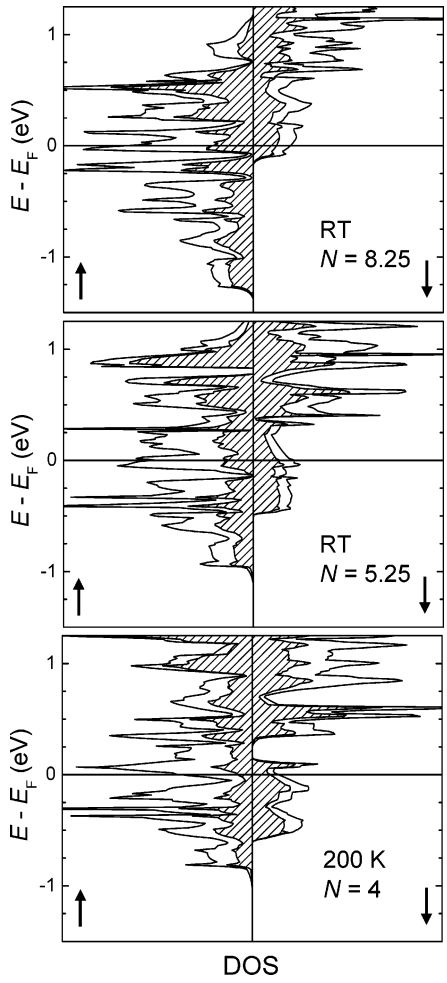

Figure 5. Total and partial DOS plots calculated for the two minimum-energy states ($N = 8.25$ and 5.25) of the RT structure and the ground state ($N = 4$) of the 200 K structure of NaV_6O_{11}. The solid lines refer to the total DOS plots, and the partial DOS plots for the V(1) atoms are indicated by shading. The partial DOS plots for the V(2) and V(3) atoms are shown in the supplementary Figure S2.

3d orbital populations calculated for the two minimum-energy states of the RT structure ($N = 5.25$ and 8.25) as well as the ground state of the 200 K structure ($N = 4$). Since the total 3d orbital populations of the three different vanadium atoms are similar, their oxidation states should be similar, so that the assumption[10] of different oxidation states for the V(1), V(2), and V(3) atoms is not supported. Nonnegligible covalent bonding interactions between the V and O atoms lead to significant O 2p/V 3d orbital mixing in the p-block and d-block bands of NaV_6O_{11}, and electron delocalization is very significant in NaV_6O_{11}, so that the oxidation state consideration on the basis of the ionic bonding scheme does not provide a useful picture.

3.3. Total and Partial Density of States. The plots of the total and partial density of states (DOS) calculated for the d-block bands of the two minimum-energy states of the RT structure ($N = 5.25$ and 8.25) and those of the ground state of the 200 K structure ($N = 4$) are presented in Figure 5, where the partial DOS plots are given only for the V(1) atoms. The partial DOS plots for the V(2) and V(3) atoms are presented in Figure S2 of the Supporting Information. On the basis of our discussion of Figures 3 and 4 as well as of Table 1, it is straightforward to understand the evolution

Table 2. Contributions of the Up-Spin and Down-Spin Electrons of the V(1), V(2), and V(3) Atoms to the DOS at the Fermi Level, $n(E_F)$, Calculated for the RT and 200 K Crystal Structures of NaV_6O_{11}[a]

		RT ($N = 8.25$)	RT ($N = 5.25$)	200 K ($N = 4$)
V(1)	up-spin	1.35	0.79	0.47
	down-spin	0.71	0.82	0.55
V(2)	up-spin	1.40	1.53	1.78
	down-spin	0.22	0.21	0.08
V(3)	up-spin	3.80	2.37	1.16
	down-spin	0.18	0.16	0.18

[a] The contributions to $n(E_F)$ are in units of states/eV per atom.

Table 3. V(1)···V(1) and V(2)···V(2) Contact Distances and Their $\langle(\Delta e)^2\rangle$ Values Calculated for NaV_6O_{11} at Temperatures above and below the Trimerization Temperature[a]

		V(1)···V(1)	V(2)···V(2)
RT	distance	2.856	2.684
	$\langle(\Delta e)^2\rangle$	15 800	15 700
200 K	distance	2.746/2.959	2.677
	$\langle(\Delta e)^2\rangle$	36 300/4000	15 200

[a] The V···V distances are in Å, and the $\langle(\Delta e)^2\rangle$ values in $(meV)^2$.

of the relative positions of the up- and down-spin d-block bands with respect to the Fermi level.

At 200 K, the spin-up and spin-down DOS plots for the V(1) atoms differ largely in shape, and the V(1) up-spin and down-spin populations do not cancel out completely below T_t. The difference in shape for the spin-up and spin-down DOS plots for the V(1) atoms arises because the up-spin and down-spin electrons engage in different exchange interactions[25] with the spins of the V(2) and V(3) atoms that remain strongly polarized. Therefore, it is incorrect to describe the trimerization of the V(1) atoms in the V_3O_8 kagomé lattice in terms of the "complete" spin pairing picture, which one arrives at by considering isolated V_3 trimers. The V_3 trimers below T_t are not isolated but interact strongly, so that no forbidden energy gap develops below T_t in the up-spin and down-spin d-block bands of the V(1) atoms. Thus, the trimerization of NaV_6O_{11} might be described as a "spin-polarized" CDW, in contrast to an ordinary CDW as found from nonmagnetic metals.

The contributions of the V(1), V(2), and V(3) atoms to the DOS at the Fermi level, $n(E_F)$, are summarized in Table 2 for the RT and 200 K structures, which shows that all the vanadium atoms V(1), V(2), and V(3) contribute to $n(E_F)$. Thus, it is understandable that NaV_6O_{11} is metallic along the parallel and perpendicular directions.[6,7] On going from RT to 200 K, the total contribution to $n(E_F)$ from V(1) is reduced by a factor of approximately 2, that from V(2) is slightly increased, and that from V(3) is reduced by a factor of approximately 3. For the V(1) contribution to $n(E_F)$, the up-spin contributes more than the down-spin at RT by a factor of 2, but the up-spin and down-spin contribute almost equally at 200 K. Since a band gap opening does not occur at the Fermi level, the probable cause for the weakly semiconducting behavior of the perpendicular conductivity of NaV_6O_{11} between 245 and 80 K should be sought from a mobility decrease of the carriers in this temperature region. It may be possible that the mobility of the down-spin electrons of V(1) along the perpendicular direction is lowered by disorder in the up-spins of V(2) and V(3) below 245 K. Once this disorder is reduced when the temperature is lowered below 80 K, the mobility would increase again so that the weakly semiconducting behavior disappears.

(25) Whangbo, M.-H.; Koo, H.-J.; Villesuzanne, A.; Pouchard, M., *Inorg. Chem.* **2002**, *41*, 1920, and the references therein.

4. Spin Pairing Tendency

Our discussion in the previous section shows that in the ground state of the RT structure of NaV_6O_{11} the V(1), V(2), and V(3) atoms each have approximately one unpaired spin and that in the ground state of the 200 K structure the V(1) site becomes close to nonmagnetic while the V(2) and V(3) sites each have one unpaired spin. Though weaker than in the trimerized state, a spin-pairing tendency is found for V(1) for the RT structure ($N = 5.25$ state). The trimerization of the V(1) atoms hardly affects the tendency for antiferromagnetic coupling for the V(2) atoms. In this section, we discuss these observations in terms of spin dimer analysis, which describes spin exchange interactions between localized spins in magnetic solids.[22] In spin dimer analysis based on EHTB calculations, the strength of antiferromagnetic interaction between two spin sites is measured by the antiferromagnetic spin exchange parameter J_{AF}, which is approximated by[22]

$$J_{AF} \approx -\frac{\langle(\Delta e)^2\rangle}{U_{eff}}$$

where the effective on-site repulsion U_{eff} is essentially a constant for a given system. The $\langle(\Delta e)^2\rangle$ term is further approximated by[22]

$$\langle(\Delta e)^2\rangle \approx \frac{1}{M^2}\sum_{\mu=1}^{M}(\Delta e_{\mu\mu})^2$$

where $\Delta e_{\mu\mu}$ is the energy split that results when two magnetic orbitals ϕ_μ on adjacent spin sites interact. The V(1) and V(2) atoms of NaV_6O_{11} are located at slightly distorted octahedral sites. Thus, a V^{3+} (d^2) cation at these sites has the electron configuration $(t_{2g})^2$, and a V^{4+} (d^1) cation has the electron configuration $(t_{2g})^1$. For simplicity, we label the t_{2g}-block levels of each spin site as ϕ_1, ϕ_2, and ϕ_3 and define the energy term $\Delta^2 = (\Delta e_{11})^2 + (\Delta e_{22})^2 + (\Delta e_{33})^2$. Then, for both V^{3+} (d^2) and V^{4+} (d^1) cations, the $\langle(\Delta e)^2\rangle$ term is written as $\langle(\Delta e)^2\rangle \approx \Delta^2/9$.[22]

The $\langle(\Delta e)^2\rangle$ values calculated for the V(1)···V(1) and V(2)···V(2) contacts in the RT and 200 K crystal structures of NaV_6O_{11} are summarized in Table 2 along with the V(1)···V(1) and V(2)···V(2) contact distances. These values are practically the same for the V(1)···V(1) and V(2)···V(2) contacts at RT, that is, the tendency for spin pairing is similar for the V(1)···V(1) and V(2)···V(2) contacts. They are practically the same for the V(2)···V(2) contact at RT and 200 K, that is, the trimerization of the V(1) atoms does not change the tendency for spin pairing in the V(2)···V(2) contact. However, the trimerization increases the $\langle(\Delta e)^2\rangle$ value by a factor of 2 for the shortened V(1)···V(1) contact but makes it negligible for the lengthened V(1)···V(1) contact. These results are consistent with the spin-pairing

tendencies of the V(1) and V(2) sites deduced from first-principles electronic band structure calculations. This shows that significant antiferromagnetic interactions exist in NaV_6O_{11}, as found from the large negative Curie−Weiss temperature (also true for SrV_6O_{11} and PbV_6O_{11}),[9] and that these interactions are of the same magnitude for V(1) and V(2) above T_t. In our first-principles calculations, the spin-pairing tendency for V(1) is found stronger even at RT, where trimerization is absent. Therefore, our spin dimer and band structure analyses indicate that the trimerization of NaV_6O_{11} is driven by both magnetic and electronic (CDW or second-order Jahn−Teller) instabilities, and the nature of the spin pairing between V(1) atoms in the kagomé lattice below T_t is closer to a diamagnetic state than to an antiferromagnetic state. This is due to the stronger pairing in the V(1)−V(1) metal−metal bonds of the V_3 trimer clusters (Figure 2b).

5. Concluding Remarks

As a function of the number of unpaired spins per FU, the total energy of the RT structure of NaV_6O_{11} has two minima at $N = 5.25$ and 8.25, which differ in energy by less than 3 meV per FU, and the total energy of the 200 K structure of NaV_6O_{11} has a minimum at $N = 4$ with the states of $N \geq 4$ lying within a small energy difference from the minimum. Consequently, states with a wide range of N values (i.e., $\sim 4 < N < \sim 9$) are expected to contribute to the magnetic properties of NaV_6O_{11} above and below the trimerization temperature T_t. The thermal populations of the "low-lying excited states" amount to gapless excitations rather than gapped excitations. The V(1), V(2), and V(3) sites of NaV_6O_{11} have a similar oxidation state, and their difference lies in the extents of their spin polarization. The unpaired spin population of the V(1) site is significantly reduced but remains nonzero below T_t. The V(2) sites of the V_2O_9 dimers in NaV_6O_{11} do not form diamagnetic pairs but possess greater than one unpaired spin per site above and below T_t. The V(3) sites of the VO_5 trigonal bipyramids possess approximately one unpaired spin per site above and below T_t. Our spin dimer analysis shows that the spin-pairing tendencies for the V(1)···V(1) and V(2)···V(2) interactions are the same above T_t and that the trimerization increases the spin-pairing tendency for the V(1)···V(1) contact by a factor of 2 but does not change the spin-pairing tendency for the V(2)···V(2) contact. Our electronic band structure and spin dimer analyses suggest that the trimerization of NaV_6O_{11} is driven by metal−metal bonding and antiferromagnetic interactions in trimer clusters.

In summary, the present work is not in support of the heuristic assumptions Kato et al.[9,10] introduced to interpret the magnetic susceptibility and ^{23}Na NMR data of NaV_6O_{11} and shows that the trimerization of NaV_6O_{11} is significantly different in nature from that of $LiVO_2$. The magnetic and transport properties of NaV_6O_{11} as well as its analogues SrV_6O_{11} and PbV_6O_{11} should be reinterpreted on the basis of the findings presented in this work. It is hoped that our work will stimulate further experimental and theoretical investigations on these fascinating systems.

Acknowledgment. The work at NCSU was supported by the Office of Basic Energy Sciences, Division of Materials Sciences, U.S. Department of Energy, under Grant DE-FG02-86ER45259. The authors thank the Pole M3PEC, Bordeaux 1 University, France, for computing resources.

Supporting Information Available: Figure S1 of the two distinct ΔE-versus-N curves calculated for the 200 K structure of NaV_6O_{11} and Figure S2 of the partial DOS for V(2) and V(3) (word/PDF). This material is available free of charge via the Internet at http://pubs.acs.org.

CM050666Y